



Role of the microstructure on the magnetic properties of Co-doped ZnO nanoparticles

B. Martínez, F. Sandiumenge, Ll. Balcells, J. Arbiol, F. Sibieude, and C. Monty

Citation: [Applied Physics Letters](#) **86**, 103113 (2005); doi: 10.1063/1.1880433

View online: <http://dx.doi.org/10.1063/1.1880433>

View Table of Contents: <http://scitation.aip.org/content/aip/journal/apl/86/10?ver=pdfcov>

Published by the [AIP Publishing](#)



Re-register for Table of Content Alerts

Create a profile.



Sign up today!



Role of the microstructure on the magnetic properties of Co-doped ZnO nanoparticles

B. Martínez,^{a)} F. Sandiumenge, and Ll. Balcells

Institut de Ciència de Materials de Barcelona (ICMAB-CSIC), Campus Universitari de Bellaterra, Bellaterra 08193, Spain

J. Arbiol

Serveis científics, U. de Barcelona, Diagonal 560, Barcelona 08028, Spain

F. Sibileude and C. Monty

CNRS/Institut de science et génie des Matériaux et Procédés, BP5 Odeillo, 66125-cedex Font Romeu, France

(Received 17 September 2004; accepted 19 January 2005; published online 3 March 2005)

We report on the magnetic and structural properties of Co-doped ZnO nanoparticles prepared by the vaporization-condensation method in a solar reactor. X-ray diffraction data and high-resolution electron microscopy (HREM) confirm the total absence of metallic Co clusters or any other phase different from würtzite-type ZnO. Electron energy loss spectroscopy analyses performed on several particles indicate that the oxidation state of Co is +2 and yield an average Co concentration of 4.5 at. %, in good agreement with the nominal composition. Transmission electron microscopy micrographs show that shape and size of the particles are strongly dependent on the preparation conditions, as well as the microstructure as evidenced by HREM. Ferromagnetism is only found in samples prepared in vacuum revealing a close correlation between microstructure and magnetic properties. © 2005 American Institute of Physics. [DOI: 10.1063/1.1880433]

The pursued dream of using spin degree of freedom of the charge carriers in order to increase both speed and storage capacity in microelectronic devices has stimulated the interest in the so-called diluted magnetic semiconductors (Ref. 1) due to their promising magnetic properties.^{2,3} Since the appearance of the paper by Dietl *et al.*³ predicting the existence of high-temperature ferromagnetism (FM) in some magnetically doped wide band gap *p*-type semiconductors much attention has been focused in these materials. Particularly TiO₂ (Refs. 4 and 5) and ZnO (Ref. 6) doped with different transition metals (Co, Mn, Fe, Ni, Cr, etc.) have been the subject of intense research. In addition to Dietl's theory, FM in magnetically doped ZnO has also been theoretically investigated suggesting the existence of FM ordering without additional charge carriers for V, Cr, Fe, Co, and Ni dopants.⁷

Nevertheless, in spite of the large number of papers published, there is no clear agreement about the nature of the magnetic properties of samples prepared by different methods and different groups (see Ref. 8 for a summary). Conflicting results have been reported for Co-doped TiO₂. Early works suggested segregation and the formation of Co clusters as the origin of FM signal,⁹ but more recent results seems to indicate the existence of intrinsic FM.¹⁰

Similarly, confusing results have also been reported in the case of Co-doped ZnO (Refs. 11–13) but recently room-temperature FM in single-phase Co-doped (Refs. 14 and 15) and Mn-doped (Ref. 16) ZnO have been reported.

In this work, we report on the magnetic and structural properties of Co-doped ZnO nanophase particles prepared by the vaporization-condensation method in a solar reactor. It is found that FM is extremely dependent on the preparation

conditions and only is observed in samples prepared in a vacuum. A clear correlation between the magnetic properties and the actual microstructure of the samples is found.

Co-doped ZnO nanophase particles have been prepared by the vaporization-condensation method in an evaporated chamber placed at the focus of a solar reactor in the High Flux Solar Facilities in Odeillo. The material is melted inside a glass balloon by using the sun heating power focused in the sample by means of a curve focusing mirror, vaporized, and then condensed. Depending on the atmosphere conditions inside the balloon, different shape and size particles distribution can be obtained. The targets have been prepared by using a mixture of ZnO and CoO powders (Aldrich, purity 99.99%) heated in air at 1115 °C for 12 h to obtain ceramic pellets.

Samples of ZnO with 5% molar of CoO have been prepared in a vacuum (10⁻² Torr) (Sample A) and with an air pressure of 70–100 Torr (Sample B) inside the balloon. The purity of the Zn_{1-x}Co_xO obtained particles have been tested by using x-ray diffraction (XRD), high-resolution electron microscopy (HREM), transmission electron microscopy (TEM), and electron energy loss spectroscopy (EELS). Irrespective of the pressure inside the balloon, no evidence of metallic Co clusters or any other phase different from würtzite-type ZnO have been found. In Fig. 1, we show XRD spectra for Samples A [Fig. 1(a)] and B [Fig. 1(b)]. It is evident that only the peaks corresponding to the ZnO würtzite (SG P6₃mc, *a*=0.32 nm, *c*=0.52 nm) structure are detected in both samples. EELS spectra obtained in several particles indicate that the oxidation state of Co is +2. This strengthens the idea that Co substitutes for Zn in the lattice. They also confirm that Co concentration is of about 4.5 at. %, in good agreement with the nominal composition (5% molar). This result strongly suggests the absence of Co-containing foreign phases or metallic Co clusters.

^{a)}Electronic mail: ben.martinez@icmab.es

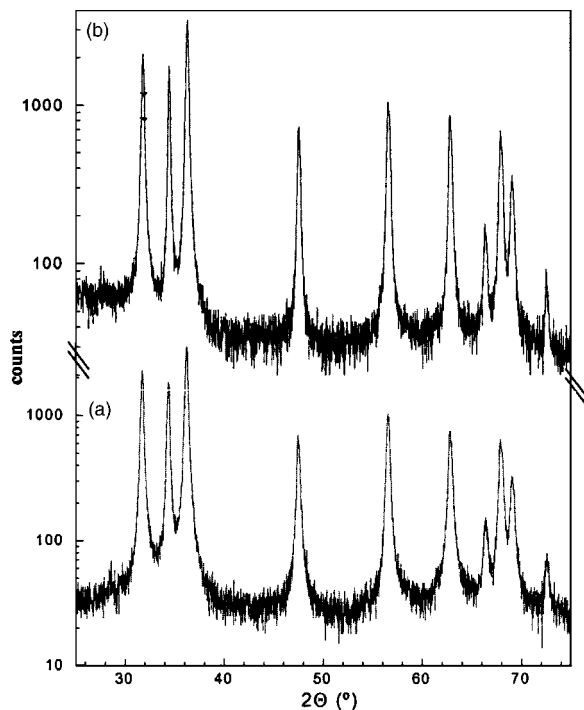


FIG. 1. XRD patterns for Samples A and B.

The magnetic properties of the samples have been studied by using a MPMS-XL7 SQUID superconducting quantum interference device (Quantum Design) magnetometer. Samples prepared in a vacuum exhibit hysteretic behavior with low coercivity (about 100 Oe) at $T=5$ K and extrapolated zero-field magnetization well below that expected for Co^{2+} in a tetrahedral crystal field ($3 \mu_B/\text{Co}$). On the other hand, samples prepared under pressure conditions are paramagnetic (see Fig. 2).

In Fig. 3, TEM micrographs corresponding to Samples A and B are shown. Tetrapodlike morphologies are recognized in both cases. Similar structures have also been reported for Mn-doped samples.¹⁷ The size of the tetrapods are markedly larger when the synthesis is performed at higher pressures

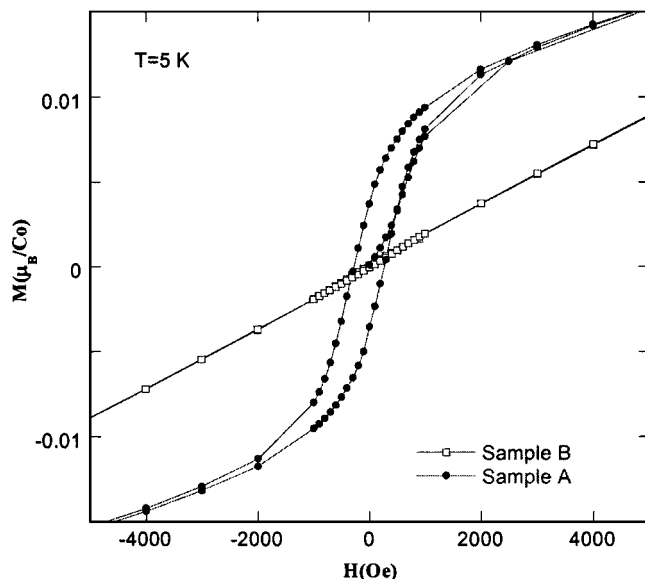
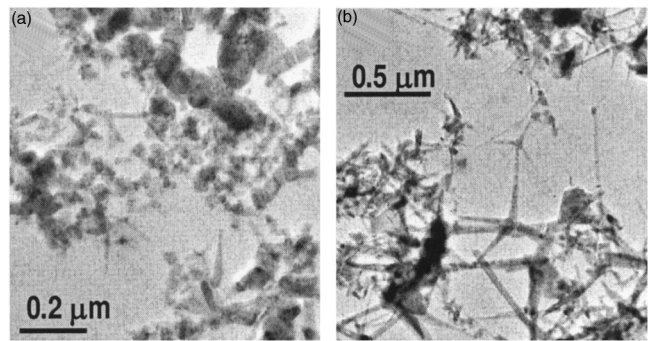
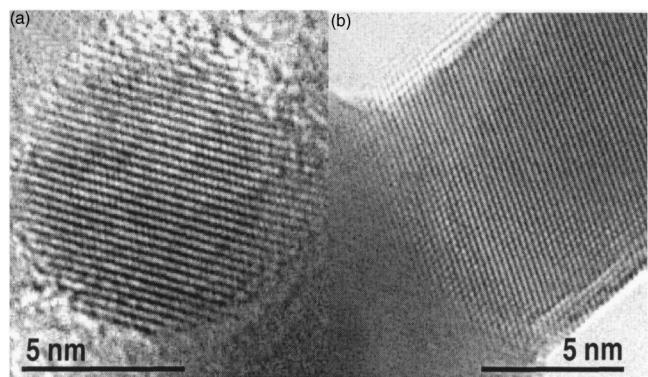
FIG. 2. $M(H)$ curves obtained at $T=5$ K for Samples A and B. The ferromagnetic character of Sample A is clearly shown.

FIG. 3. TEM micrographs corresponding to Samples A (a) and B (b). Substantial differences in the size of the tetrapods are observed.

(Sample B). Therefore, we should conclude that the growth rate along the axes of the tetrapod arms is enhanced at higher pressures. In addition, in Sample A, a large fraction of particles with rounded morphologies is also present.

In order to detect possible differences between rounded and tetrapod particles in Sample A, we have tested several particles by using HREM. In Fig. 4, we presents high-resolution image of a rounded particle [Fig. 4(a)] and a part of a tetrapod arm [Fig. 4(b)]. In both cases, the images exhibit homogeneous defect free crystal lattices corresponding to ZnO. The contrast variation observed in the image of the tetrapod arm [Fig. 4(b)] is associated with a thickness variation.

Conversely, HREM images of Sample B indicate that defective structures develop within the tetrapod arms, likely due to the higher growth rate of the crystallites. An example is shown in Fig. 5, corresponding to a part of a tetrapod arm. The image exhibits a patchedlike contrast distribution. The Fourier transform patterns, shown as insets corresponding to the boxed areas, are positioned in regions exhibiting significant contrast differences. Intensity profiles taken across the (01-10) and (0-110) pairs of spots indicate that the width of the intensity distribution around the spots is increased in the boxed area exhibiting a defective contrast, thus signalling the occurrence of slightly strained regions within the ZnO matrix. Such weak stress sources are tentatively attributed to the existence of a non-homogeneous Co distribution with small (<5 nm) Co-rich areas within the ZnO matrix. The occurrence of such defective regions is clearly correlated with the higher growth rates of the crystallites grown at higher pressures, since they are not found in Sample A, and indicate a

FIG. 4. HREM image of a rounded particle (a) and a tetrapod arm (b) corresponding to Sample A, viewed along the $[20\bar{2}\bar{1}]$ and $[\bar{1}011]$ directions, respectively.

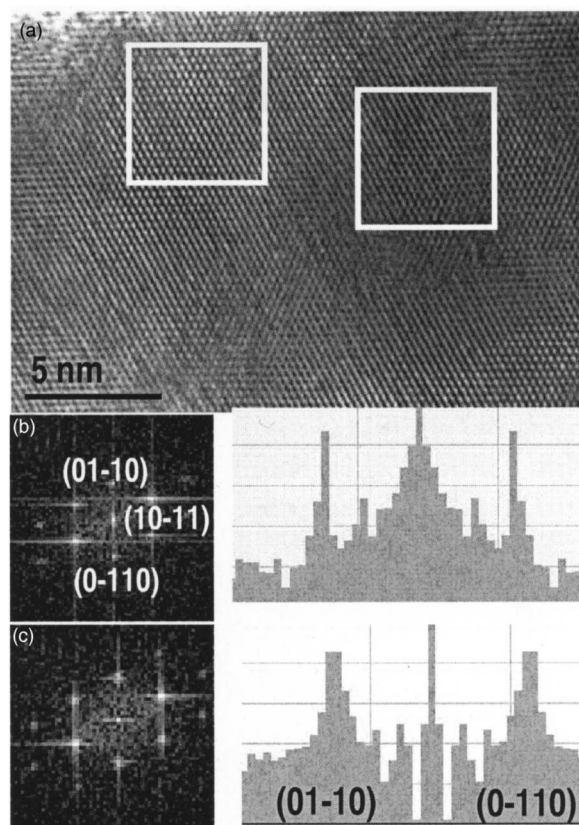


FIG. 5. HREM image of a tetrapod arm of Sample B, observed along the $[-1011]$ zone axis (a). The existence of a defective structure is shown. (b) and (c) The fast Fourier transform spectra of boxed areas, along with their vertical intensity profiles taken through the origin, emphasizing lattice distortions.

nonhomogeneous Co distribution. Thus, microstructural differences between Samples A and B offer a very reliable explanation of the observed magnetic behavior. While Sample A exhibits a very uniform microstructure, with a homogeneous distribution of Co atoms, Sample B has a defective microstructure due to a much faster growth rate. This fact implies that, assuming a mean field model (Ruderman–Kittel–(Kasuya)–Yosida RKKY interactions),³ mean distances between Co atoms in Sample A should favor FM interaction, as it is in fact observed. On the contrary, the defective microstructure found in Sample B indicates a nonhomogeneous Co distribution with small Co-rich areas within the ZnO matrix in which AF interactions are enhanced due to shorter distances between Co atoms.

In summary, we have demonstrated that intrinsic magnetic properties of Co-doped ZnO are intimately connected to the actual microstructure of the samples. Our TEM studies

show that particles of Sample B are larger than those in Sample A due to a much faster growth rate because of different pressure conditions in the evaporation chamber. HREM studies demonstrate that faster growth rate implies a defective microstructure with small Co-rich areas in the ZnO matrix, i.e., distances between Co atoms in these areas are shorter reinforcing antiferromagnetic interactions. Co atoms not included in these areas are far apart and give place to the observed paramagnetic behavior. Sample A exhibits a uniform microstructure with a more homogeneous distribution of Co atoms in the ZnO matrix in which mean Co–Co distances favor FM interactions giving place to the observed FM ordering.

The authors acknowledge financial support from the MCyT (Spain) and FEDER. Projects MAT2002-04551-C03-01 and MAT2003-04161, and CEE-SOLFACE project.

¹See for example S. J. Pearton, C. R. Abernathy, D. P. Norton, A. F. Hebard, Y. D. Park, L. A. Boatner, and J. D. Budai, *Mater. Sci. Eng.*, **R**, **40**, 137 (2003).

²H. Ohno, *Science* **281**, 951 (1998).

³T. Dietl, H. Ohno, M. Matsukura, J. Cibert, and D. Ferrand, *Science* **287**, 1019 (2000).

⁴S. A. Chambers, *Mater. Today* **5**, 34 (2002).

⁵Y. Matsumoto, M. Murakami, T. Shono, T. Hasegawa, T. Fukumura, M. Kawasaki, P. Ahmet, T. Chikyow, S. Koshikara, and H. Koinuma, *Science* **291**, 854 (2001).

⁶T. Fukumura, Z. Jin, A. Ohtomo, H. Koinuma, and M. Kawasaki, *Appl. Phys. Lett.* **75**, 3366 (1999).

⁷K. Sato and H. Katayama-Yosida, *Semicond. Sci. Technol.* **17**, 357 (2002).

⁸T. Fukumura, Y. Yamada, H. Toyosaki, T. Hasegawa, H. Koinuma, and M. Kawasaki, *Appl. Surf. Sci.* **223**, 62 (2004).

⁹P. A. Stamp, R. J. Kennedy, X. Yan, and J. S. Parker, *J. Appl. Phys.* **92**, 7114 (2002); S. A. Chambers, T. Droubay, C. M. Wang, A. S. Lea, R. F. C. Farrow, L. Folks, V. Deline, and S. Anders, *Appl. Phys. Lett.* **82**, 1257 (2003).

¹⁰S. R. Shinde, S. B. Ogale, S. Das Sarma, J. R. Simpson, H. A. Drew, S. E. Lofland, C. Lanci, J. P. Buban, N. D. Browning, V. N. Kulkarni, J. Higgins, R. P. Sharma, R. L. Greene, and T. Venkatesan, *Phys. Rev. B* **67**, 115211 (2003); A. Manivannan, G. Glaspell, and M. S. Seehra, *J. Appl. Phys.* **94**, 6994 (2003); T. Zhao, S. R. Shinde, S. B. Ogale, H. Zheng, T. Venkatesan, R. Ramesh, and S. Das Sarma (unpublished).

¹¹T. Fukumura, Z. Jin, M. Kawasaki, T. Shono, T. Hasegawa, S. Koshihara, and H. Koinuma, *Appl. Phys. Lett.* **78**, 958 (2001).

¹²S. W. Jung, S. J. An, G. C. Yi, C. U. Jung, S. I. Lee, and S. Cho, *Appl. Phys. Lett.* **80**, 4561 (2002).

¹³A. Tiwari, C. Jin, A. Kvit, D. Kumar, F. J. Muth, and J. Narayan, *Solid State Commun.* **121**, 371 (2002).

¹⁴L. Yan, C. K. Ong, and X. S. Rao, *J. Appl. Phys.* **96**, 508 (2004).

¹⁵S. Ramachandran, A. Tiwari, and J. Narayan, *Appl. Phys. Lett.* **84**, 5255 (2004).

¹⁶P. Sharma, A. Gupta, K. V. Rao, F. J. Owens, R. Sharma, R. Ahuja, J. M. Osorio, B. Johansson, and G. A. Gehring, *Nat. Mater.* **2**, 673 (2003).

¹⁷V. A. L. Roy, A. B. Djuricic, H. Liu, X. X. Zhang, Y. H. Leung, M. H. Xie, J. Gao, H. F. Lui, and C. Surya, *Appl. Phys. Lett.* **84**, 756 (2004).